

Damping Modelling in Transformer Energization Studies for System Restoration: Some Standard Models Compared to Field Measurements

M. Martínez Duró

Abstract-- This paper deals with damping modeling for transformer energization studies for system restoration purposes. A review of some of the literature recommendations for these studies is presented. Then, several damping models for generators, lines and transformers are benchmarked by means of simulation vs. field test measurements comparison.

For the field test case considered, results show that simple models are as accurate as the more sophisticated frequency-dependent ones. A technique for automatized benchmark has been used that could be applied to other field test cases in order to draw general conclusions.

Index Terms-- Power system transients, Power transformers, Power system modeling

I. INTRODUCTION

A. Power System Restoration, Transformer Energization and Temporary Overvoltages

After a complete or partial blackout, power system restoration involves energizing no-load transformers, either transmission system transformers or auxiliary transformers of power plants.

On the one hand, in system restoration circumstances, energization is done from a weak network (i.e., made of few available power plants, few long transmission lines, poorly meshed) with little or no load; thus the network has high harmonic impedance at low frequencies and little damping. On the other hand, transformer magnetizing inrush current can be very high, reaching values as high as several times the rated current, and contains low frequency harmonics. As a consequence of these two factors, harmonic temporary overvoltages can appear and damage network equipment [1][3][4].

These Temporary Overvoltages (TOV) are low-frequency (below 1 kHz), long duration (up to several seconds) and weakly damped voltage waves [5]. Since TOV withstand capability of equipment is a function not only of amplitude but also duration of the stress [6], correct representation of damping is a critical parameter in simulation studies. On the one hand, overdamping modeling gives underestimated constraints, what could lead to equipment damage. On the other hand, underdamping modeling overestimates constraints and therefore can lead to oversizing protection systems or to unduly forbid specific operation schemes.

B. Making Modelling Choices: Literature

Several international working groups have established recommendations on modelling each of the network components in TOV studies [7][8][9][10].

Nevertheless, engineers have often to deal with multiple choices. In some cases, several models are available for some network components, in spite of their different degree of complexity; the simpler but accurate enough model should be chosen. In other cases, available data don't permit the implementation of recommended models.

For instance, whereas an important effort has been made in transformer modelling to develop topologically correct core models necessary for specific studies like ferroresonance [11][12], many usual network configurations might be studied with simpler models not taking into account the real core topology of transformers [10] (§II.A). Compared to the later model, the former needs more data, not always easily available, and its implementation is more time-consuming. Thus, it is important for the engineer to make the good choice.

Similarly, whereas in some cases automatic voltage regulation (AVR) has to be modelled, [7] (§4) states that its effect is not important in general. Again, the engineer needs to make the good choice depending on whether AVR is important or not in the studied case.

C. Validating Modelling Choices: Field Tests vs. Parametric Simulations

A particular study involves making good modelling choices, those that provide enough accuracy with the least complexity. These choices are made by taking into account literature generic recommendations and previous experience in similar cases.

Nevertheless, only field tests of the studied configuration can provide a final validation of modelling choices. Comparison between field measurements and simulation results will say if selected models are accurate enough to reproduce involved physical phenomena.

This comparison, though, is not an easy task. Many network parameter values can be unknown or known with some uncertainty. And depending on the physical phenomena involved, simulation results can be very dependent on values assigned to these parameters.

In transformer energization studies, critical parameters roughly known include, among others, high saturation characteristic and residual fluxes of transformers, circuit-breaker switching times, upstream network harmonic impedance [8]. For instance, a 10% variation of the final slope of the saturation curve of a transformer can lead to totally different inrush currents and thus totally different harmonic overvoltages.

The effect of parameter value uncertainty has to be taken into account when comparing field measurements to simulation results. Not doing so, wrong conclusions could be

drawn because model effects would be mixed with parameter value effects. For instance, a model could show a good agreement with measurements only for a specific (arbitrarily chosen) set of parameter values, but not for others.

Thus, in order to draw conclusions from measurements vs. simulation comparison, one needs to assess the sensitivity of the agreement to parameter values. This paper presents a technique to do so.

D. This paper: some standard models compared to field measurements

In this paper we compare performances of some usual models in transformer energization studies, paying special attention to damping modelling (which is, as we have seen, a key factor of TOV effects). These models are compared to field measurements for a real test case through a technique that takes into account the problem of the sensitivity of the agreement to parameter values.

II. FIELD TEST CASE

Field test configuration used to benchmark models is represented in Fig. 1. The auxiliary (UAT) and the main (UMT) transformers of a power plant unit are energized simultaneously.

Unit auxiliary transformer is a three-phase three-winding 58 MVA – 24/6.8 kV, Ydd11. Unit main transformer is made of 3 single-phase units 3x360 MVA – 225/24 kV, Yd11 connected.

Upstream network is made up of the sending plant, including a generator and a step-up transformer, a 48.5 km 400 kV overhead line and a 3x357 MVA – 400/225 kV autotransformer (AT). This AT has been energized before the energization of UMT+UAT.

Power frequency is 50 Hz. Measurements include voltages and currents at the HV side of the UMT terminals. Maximum peak current measured was 2200 A. No significant overvoltage was recorded.

Upstream network seen from target UMT transformer has a parallel resonance at 500 Hz.

benchmarked. The circuit breaker is modelled by three ideal switches.

A. Generator models

Three different models are benchmarked for the synchronous generator of the sending power plant.

First, a “static model” consisting in a voltage source behind the subtransient inductance of the generator, L_d'' [14] (§8). A resistance is added to this representation in series with the inductance, whose value leads to two possibilities. In the first generator model, this resistance is calculated to represent subtransient time constant, T_d'' . We are noting this resistance R_d'' .

In the second generator model, the resistance of the “static model” represents armature winding resistance, R_a [15].

Thirdly, a “dynamic model” representing Park’s equations and thus able to represent subtransient, transient and synchronous behaviour of the machine [14] (§8).

It has to be emphasized that none of the three models includes voltage regulation.

On the one hand, the “dynamic model” accounts for frequency dependency of generator inductance, whereas “static models” do not. Reference [7] (§4) acknowledges both static and dynamic models.

On the other hand, first and second models differentiate in their resistance value. The ratio between R_d'' and R_a is about 10. This means that generator contribution to global damping will be very different depending on which static model is used.

B. Overhead-lines

Two line models are benchmarked: cascaded PI-sections of constant lumped parameters calculated at power frequency, and frequency dependent distributed parameter model (EMTP “FD model”) [16][14]. Reference [7] (§4.1) acknowledges both of them.

For TOV studies, the main difference between the two models is frequency-dependent losses. Indeed, higher losses due to harmonic currents in overhead lines could have a significant impact on the overall damping.

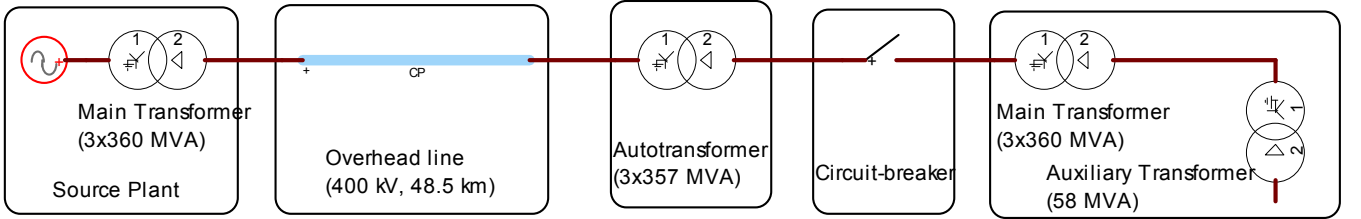


Fig. 1. Field Test Case

III. BENCHMARKED MODELS

Network elements to be modelled are: the generator, the line and the transformers. For each element, several standard models, easily accessible in EMTP-like programs, are

C. Transformers load losses as a function of frequency

All the transformers are modelled by means of single-phase star-equivalent circuits, i. e., the EMTP Saturable Transformer Component [10]. Winding resistances and leakage inductances are calculated from standard short-circuit tests [17] (§III.B) assuming they are equally shared between the windings for

two-winding transformers [14] (§6.2). When DC winding resistances are available, they are used to determine the real resistance ratio between windings [13] (§II.A).

Non-linear saturation core characteristic is included, constructed from the no-load factory tests (for the knee point) and the air-core reactance provided by the manufacturer [17]. Core losses are modelled by a constant resistance obtained from the standard no-load test, a model good enough below 1 kHz [22].

Auxiliary transformer (UAT) is a three-phase unit (one single core) but delta secondary windings allow an equivalent single-phase modelling [11] (§II.D) [14] (§6.2).

Winding resistances are modified in order to include frequency dependent load losses, as explained below.

Energization magnetizing currents can be as high as several times the rated current of the transformer. These currents contain rich low frequency harmonics. Load losses are due to this current and they are frequency-dependent. Thus, care has to be devoted to load losses modelling when dealing with transformer energization studies [7] (§4.2).

Load losses are due to eddy currents and skin effect in windings, and to stray losses [18][19]. These losses are proportional to square of the windings currents; hence they can be modelled by the winding resistances. Frequency dependence of these resistances can be expressed as [17]:

$$R(f) = R_{DC} + \Delta R_{AC} \cdot \left(\frac{f}{f_0} \right)^n \quad (1)$$

where f_0 is the power frequency.

In order to easily include frequency dependent load losses, parameters of expression (1) need to be determined for each transformer: R_{DC} , ΔR_{AC} and n . We present here a simple method for this task.

Reference [21] provides winding time-constants as a function of frequency for several transformer's rated power values; assuming a constant leakage inductance in the TOV frequency range, winding resistance can therefore be calculated as a function of frequency, $R(f)$. These values could then be used to determine R_{DC} , ΔR_{AC} and n in expression (1).

But we will be using a simpler method. Winding resistances at power frequency, $R(f_0)$, are known from standard short-circuit factory tests (see above). Sometimes, DC winding resistances, $R(0)=R_{DC}$, are also known. Then, these two values of $R(f)$ allow to fit expression (1) provided an assumption is made on the value of parameter n . Reference [17] suggests that the factor n is between 1.2 and 2, whereas [20] puts $n=2$. Here we will be using this method assuming $n=2$.

Three load loss models are benchmarked. First, a power frequency (50 Hz) losses model, where winding resistances are constant and calculated from standard short-circuit tests.

Second, a frequency-dependent load loss model, where winding is modelled by a 1 cell Foster equivalent [19], shown in Fig. 2, that fits expression (1) with $n=2$ (L_p takes leakage inductance value).

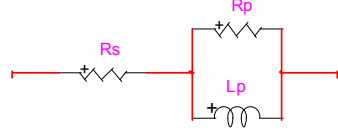


Fig. 2. Foster 1 cell equivalent

Third, an averaged constant resistance model, where winding resistance is constant but increased to account for greater losses due to harmonics; here, resistance is calculated as follows:

$$R' = 0.9 \cdot R(f_0) + 0.1 \cdot R(f_r) \quad (2)$$

where f_0 is the power frequency (50 Hz), f_r is the first positive sequence resonance frequency of the upstream network (here, 500 Hz), and $R(f)$ is calculated with (1).

IV. BENCHMARKING METHOD

A. Network models

For each element of the network, we have several alternative models: 3 for the generator losses/dynamics, 2 for line losses, 3 for transformer load losses. Thus, there are $3 \times 2 \times 3 = 18$ possible network modelling schemes which have to be simulated and compared to measurements.

B. Statistical network parameters

However, managing real test measurements makes it more complicated. As stated before, simulation results can be very sensitive to some parameters of the field test network that are not known precisely. Benchmarking method has to be able to differentiate two types of discrepancies between simulation and field measurements: those due to a bad model and those due to bad parameter values. Thus, these parameters cannot be assigned deterministic values. Instead, they are statistical parameters that are assigned several values within their accuracy range.

Statistical network parameters taken into account are the following:

- Saturation curve of transformers is built up from manufacturer approximate data. The main parameter of these curves is air-core inductance. Besides manufacturer value, L_0 , this parameter is assigned two other values at $\pm 10\%$.
- Residual flux at energized transformers, UMT+UAT. Residual flux is calculated by integrating UMT voltage at disconnection prior to energization. As voltages are noisy, the result of this calculation is not supposed to be exact. Besides the integrated values, two other values are considered at ± 0.1 pu.
- Closing times of the circuit breaker. They are determined by examination of measurements of voltages and currents. As the exact time of closing can have a big influence on simulation results, calculated closing times are supposed to be known with a 1.5 ms accuracy. For each phase, besides

the calculated values (t_i , $i=A,B,C$), two other values are considered : $t_i \pm 0.75$ ms and $t_i \pm 1.5$ ms. Thus 125 closing times combinations are considered.

Finally, the total number of simulations to be performed and compared to field measurements is obtained from the combination of network elements models to be benchmarked (18) and the network parameters values to be considered: $18 \times 3 \times 3 \times 125 = 20250$ simulation cases.

C. Criteria for automated simulation-versus-measurement comparison

Obviously, the simulation of the 20250 possibilities and subsequent comparison to field measurements cannot be done manually but has to be automated.

For this, each simulation corresponding to a combination of models and network parameters is assigned a single figure that characterizes its agreement with the field measurements, i. e., each simulation case is assigned a “distance” between simulation and measurement: thus, for a given simulation case, the minor the distance value, the better the agreement with the measurements.

This distance can be calculated in many ways depending on the data type used in the comparison (voltages, currents, or both) and the mathematical treatment given to the data (raw data versus time, frequency-spectrum analysis...).

Concerning data type, we will be using line currents at the HV terminals of the target UMT, for three reasons. Firstly, recorded voltages do not contain much meaningful information because no significant overvoltage occurred in our field test. Secondly, harmonic overvoltages due to transformer energization are very dependent on upstream network parameters that determine the impedance-vs-frequency characteristic, $Z(f)$: i. e., for similar inrush currents, little differences between real and modelled $Z(f)$ characteristic could lead to big differences in resulting overvoltages. Thirdly, our concern here is to evaluate damping modelling, and that can be assessed by current analysis, thus avoiding problems of voltage analysis.

Concerning the mathematical treatment given to data before comparison, we will be using envelopes instead of raw current-vs-time data. Envelopes are defined by local maxima and minima in a 10 ms sliding window. Since our concern is on damping modelling, envelopes contain all the desired information. This way we avoid problems of raw data-vs-time comparison, where little phase-angle differences between compared curves can lead to big differences in point-by-point distance calculation (see below).

Finally, the distance is defined as the mean root square of the sum of the point-by-point quadratic differences, as follows. For a given simulation curve, the envelope of the inrush current in each phase is calculated, $i_{s,k}$ ($k=a, b, c$). The same is done for the measured currents, $i_{m,k}$. For phase k , the distance between one simulation case and the field measurements is calculated as:

$$d_{ik} = \sqrt{\frac{1}{n} \sum_{k=1}^n (i_{s,k} - i_{m,k})^2} \quad (3)$$

where n is the number of points of the curve. Then, the single figure characterizing the simulation case is calculated as the mean value for the three phases:

$$d = \frac{1}{3} \cdot (d_{ia} + d_{ib} + d_{ic}) \quad (4)$$

Current envelopes are calculated for the first 1.5 s after energization (afterwards, currents are below the sensitivity threshold of the measuring equipment).

A MATLAB program has been implemented to manage the whole process: building up the input files for EMTP, launching the simulations, recovering the output results, calculating the distances and drawing the figures for analysis.

V. RESULTS

The automated algorithm provides the user with an array of 20250 distances. This array permits to assess the effect of a network model on the agreement between simulation and field measurements.

It also permits to evaluate the effect of statistical network parameter values. Because we are interested in network models performance and not in statistical network parameters, we first need to discard all values that lead to a bad agreement.

A. Discarding bad network parameter values

As explained before, statistical network parameters are transformer air-core inductance (3 values), transformer residual flux (3 values) and circuit-breaker switching times (125 values).

Fig. 3 shows the distance distributions for the 125 circuit-breaker switching times. Each curve corresponds to a given set of 3-phase switching times. The figure has no legend because of the number of curves and because we won't be dealing with specific switching times.

Some general explanation is needed here about these distance distributions. Each curve in Fig. 3 corresponds to those elements of the distance array associated to simulation cases where that switching time has been used. Thus, each curve contains $20250/125=162$ points.

Each point of a given curve corresponds to the distance between field measurements and a particular combination of network models and statistical network parameters. I. e., each point of a given switching time curve correspond to the distance obtained with that switching time and with a particular generator model, a particular line model, a particular transformer losses model, a particular air-core inductance value and a particular residual flux value.

The left-most point of each curve gives the minimum distance, i. e. the best simulation/measurement agreement one can obtain with that particular switching time.

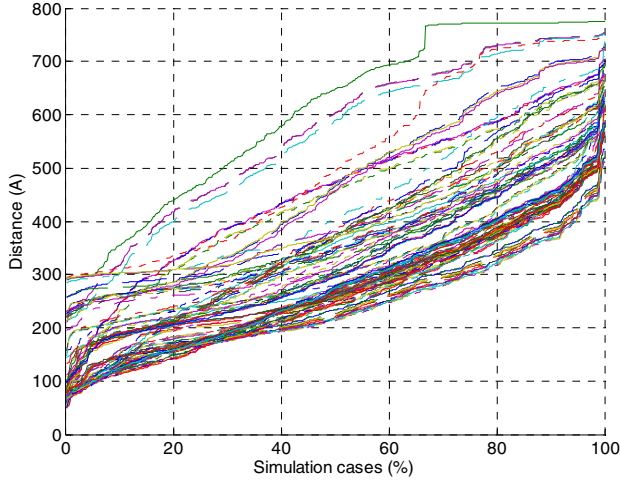


Fig. 3. Distance distributions for CB switching times

One can see in Fig. 3 that minimum distances vary between 50 A and 300 A. Switching times leading to big minimal distances can be discarded for the rest of the analysis: the poor agreement they provide means that they are far from real switching times.

Here, we discard switching times leading to distances bigger than 120 A, this is, 27 switching times out of 125. The 98 switching times left are associated to a more or less good agreement, so one cannot discriminate between them. The distributions of this set are shown in Fig. 4.

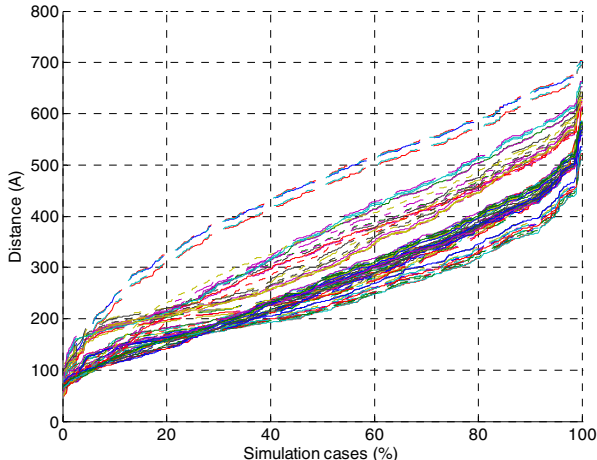


Fig. 4. Distance distributions for selected CB switching times

The same analysis is made with distance distributions of each residual flux, shown in Fig. 5.

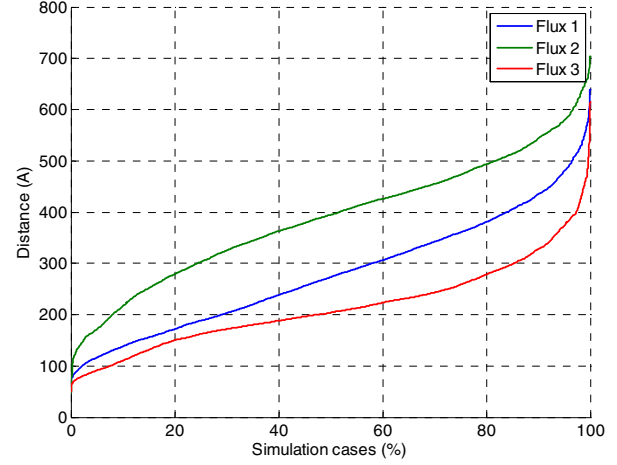


Fig. 5. Distance distributions for residual flux values

One of the residual flux values leads to much bigger distances than the other two. Nevertheless, minimal distances obtained with the three residual flux values are near, as shown in the zoom in Fig. 6, thus one cannot discard any of the values.

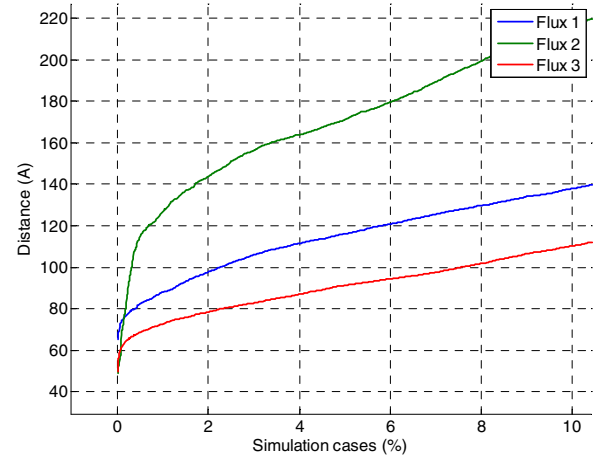


Fig. 6. Distance distributions for residual flux values (zoom)

Finally, Fig. 7 shows distance distributions obtained with the three air-core inductance values. One can see that distances obtained with high air-core reactances ($L_0+10\%$) are always higher than distances obtained with medium (L_0) or low values ($L_0-10\%$). But the difference does not seem big enough to discard any air-core reactance value.

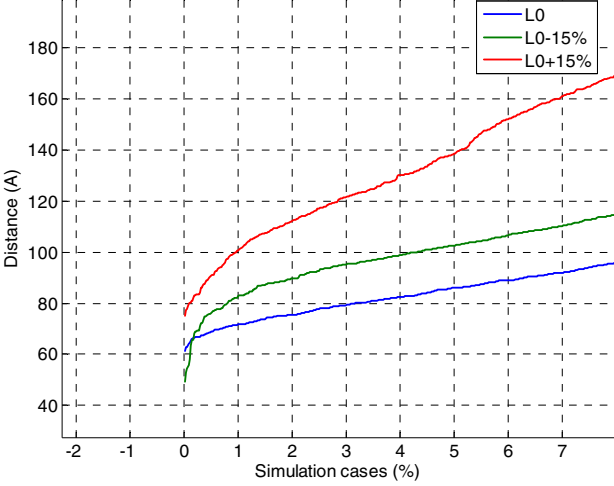


Fig. 7. Distance distributions for transformers air-core inductance (zoom)

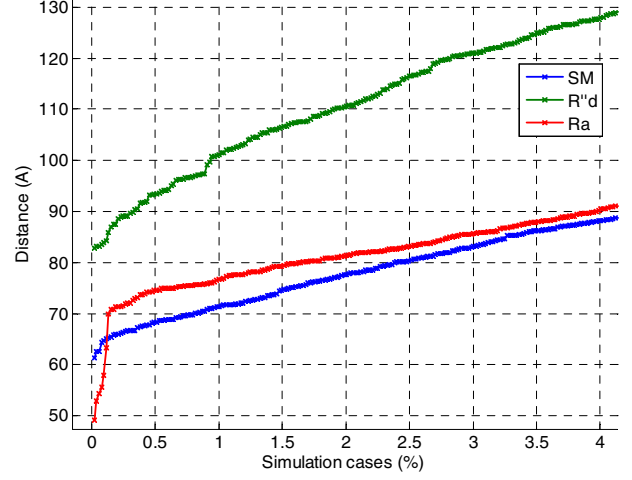


Fig. 9. Distance distributions for generator models (zoom)

B. Network models performance

Network elements for which several models are benchmarked are the generator, the overhead-line and the transformer load losses.

Distance distribution for the three **generator models** is shown in Fig. 8, with a zoom in Fig. 9. One can see that the static model with R_a (labeled “ R_a ”) and the dynamic model (Park’s equations) (labeled “SM”) lead to similar agreement, respective minimum distances being 49 A and 59 A. The static model with $R''d$ (labeled “ $R''d$ ”) leads to a bigger distance (83 A), thus worse agreement between simulation and measurements.

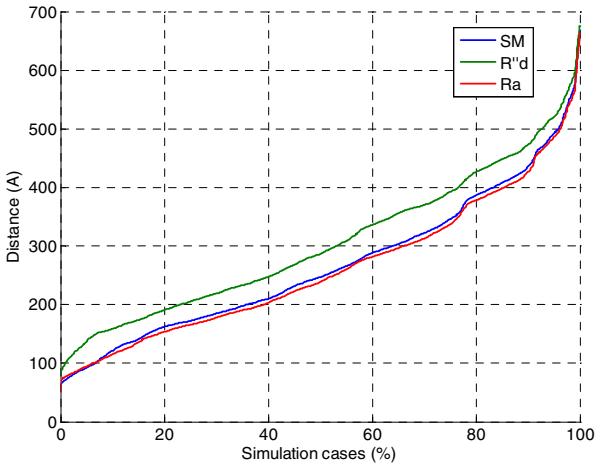


Fig. 8. Distance distributions for generator models

Fig. 10 shows, for one phase current, the envelopes of the field test measurement and of the best simulation cases for each of the three generator models. One can see that agreement is very good with the R_a static model, fairly good with the SM model and quite bad with the static $R''d$ model. Nevertheless, this figure is just illustrative, as agreement is different for the other two phases.

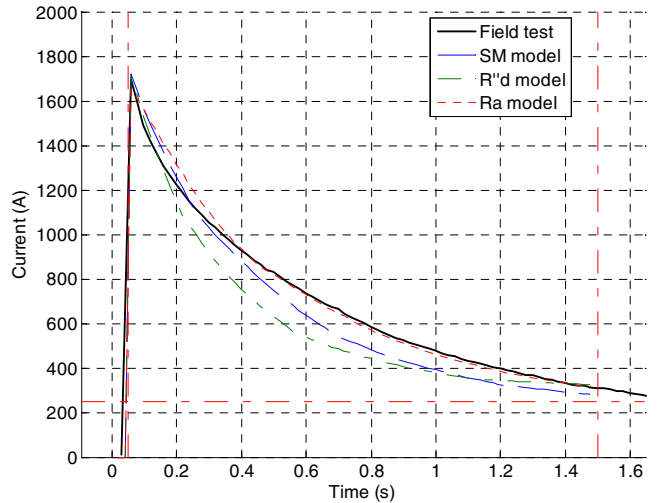


Fig. 10. Envelopes of field-test measurement and best simulation case with each of the three generator models

The effect of generator inductance uncertainty was also analyzed. With the static R_a model, three values were compared: the nominal value used before, L_g , and two other values at $\pm 15\%$. Fig. 11 shows the obtained distributions, where no significant difference is observed. Little variations of generator inductance can be of great importance when resonance occurs, but that did not happen in our field test case, where no resonant overvoltage was recorded.

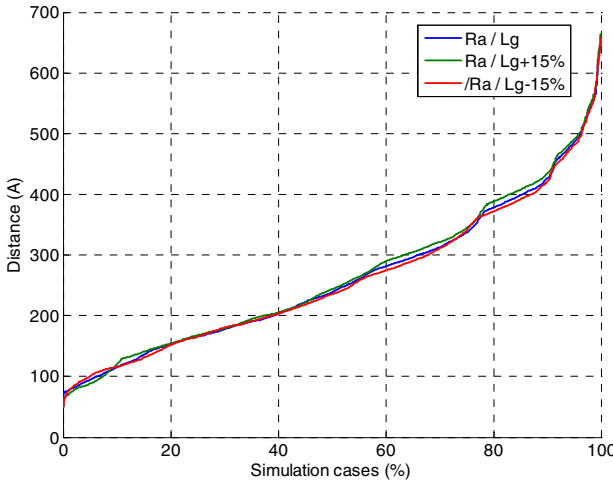


Fig. 11. Distance distributions for three generator subtransient inductance values (static R_a model)

Concerning **overhead-line modeling**, Fig. 12 shows that there is no significant difference between the two models: PI cells calculated at power frequency (50 Hz) and the frequency-dependent line model lead to a similar agreement, minimum distances being 49 A in both cases.

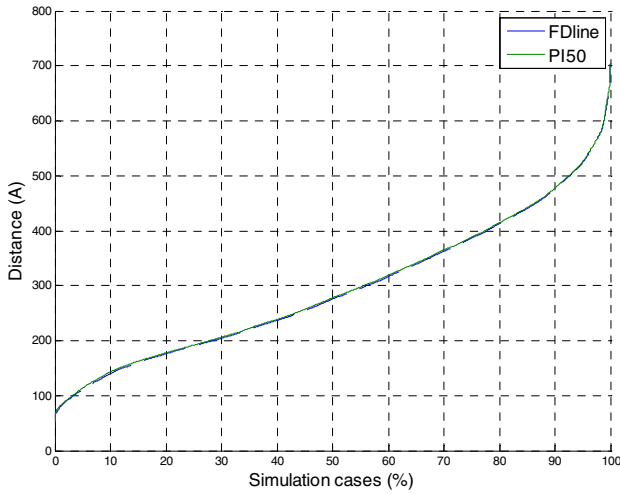


Fig. 12. Distance distributions for line models

Finally, Fig. 13 shows distance distributions associated to the three **transformers load-loss models**. Clearly, the model where winding resistances are constant but increased to account for bigger losses due to harmonics (labeled “ $R_{avg}(f_0,fr)$ ”) is very poor compared to the other two models. Indeed, the zoom on Fig. 14 shows that best agreement with this model leads to a distance of 132 A, whereas the other two models lead to a distance of 50 A.

Furthermore, this figure shows that there is no clear advantage in using the Foster equivalent (labeled “ $R(f)$ -Foster”) compared to the power frequency loss model (labeled “ $R-f0$ ”). Of course, the performance of a frequency-dependent loss model can be improved by means of a better expression

$R(f)$ and/or a better fitting and/or a better equivalent (for instance, a 2-cell Foster circuit). But that would demand more data and/or would be a more complex and time-consuming task.

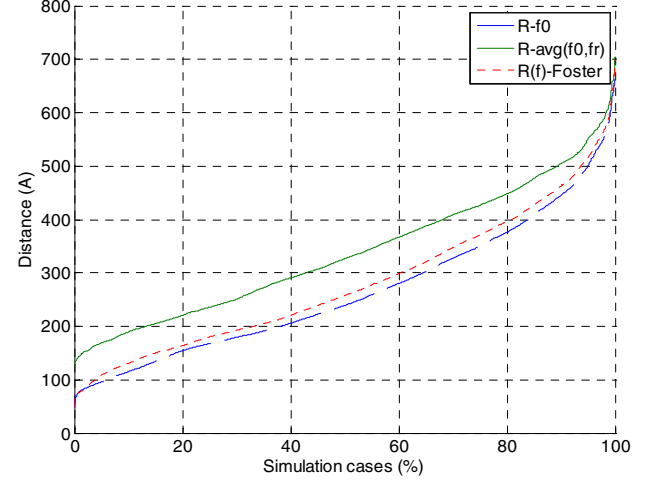


Fig. 13. Distance distributions for transformer load-loss models

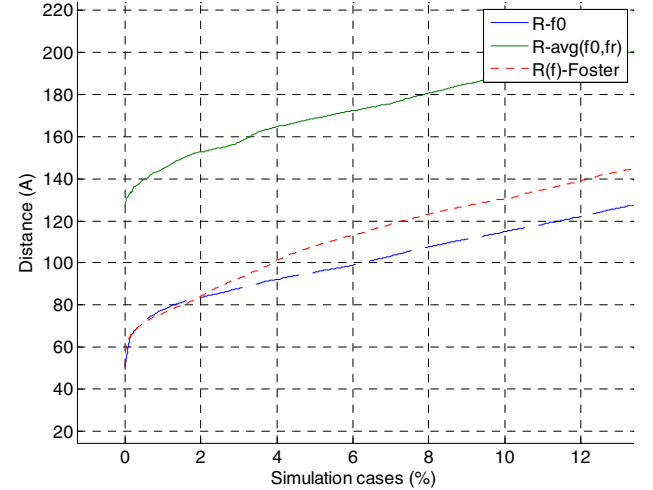


Fig. 14. Distance distributions for transformer load-loss models (zoom)

Fig. 15 shows the envelopes of the field test measurement and the best simulation cases obtained with each of the three transformer load-loss models. This figure is illustrative of the results obtained with the distance distribution analysis. In particular, one can see that the “ $R_{avg}(f_0,fr)$ ” model, because of the big losses it introduces, leads to a very bad agreement.

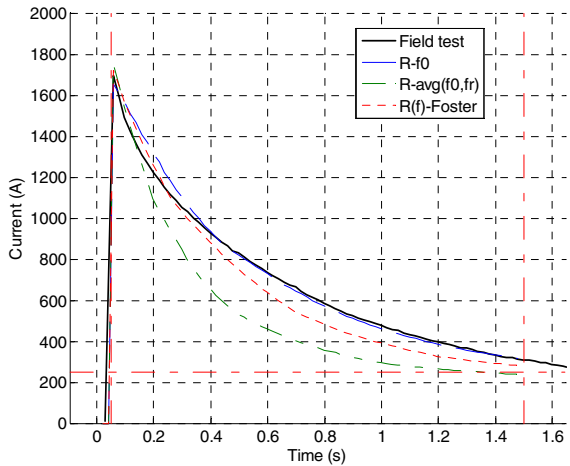


Fig. 15. Envelopes of field-test measurement and best simulation case (transformer load-loss models)

VI. CONCLUSION

This paper deals with damping modelling for transformer energization studies. A review of some of the literature recommendations for these studies has been presented. Several damping models for generators, lines and transformers have been benchmarked by means of simulation vs. field test measurements comparison. Model benchmarking method takes into account network parameters inaccuracies in order to be able to discriminate the effects of models from the effects of parameter values.

Results show that: a) A simple static generator model containing an ideal voltage source can be as accurate as a dynamic model implementing Park's equations; b) Cascaded PI cells with constant parameters lead to similar results than frequency dependent line models; c) Transformer power-frequency losses can be a good approximation of losses during the inrush transient.

Nevertheless, these results are only indicative and cannot be generalized. Indeed, despite of the benchmarking method taking into account parameter inaccuracy, other network configurations could lead to different phenomena (like different current spectrum) and thus to different results.

In order to achieve general conclusions, the same benchmarking technique should be used with other field test cases, especially with different network configurations (e. g., longer overhead-lines, higher inrush currents...).

VII. ACKNOWLEDGMENT

The author gratefully acknowledge the contribution of B. Caillault, F.-X. Zgainski and V.-L. Renouard from EDF DTG, who performed field measurements and provided initial modelling.

VIII. REFERENCES

- [1] D. Povh, Schultz W, "Analysis of overvoltages caused by transformer magnetizing inrush current", IEEE Transactions on Power Apparatus and Systems, 1978, 97(4): 1355-1365.
- [2] L. F. Blume, G. Camilli, S. B. Farnham and H. A. Peterson, "Transformer magnetizing inrush currents and influence on system operation" AIEE Trans. Power App. Sys., 63, pp. 366-375, Jan 1944.
- [3] M.M. Adibi, R.W. Alexander, and B. Avramovic, "Overvoltage control during restoration", IEEE Transactions on Power Systems, Vol. 7, No. 4, pp. 1464-1470, November 1992.
- [4] J. W. Feltes & C. Grande-Moran, "Black Start Studies for System Restoration", Power System Dynamic Performance Committee, 2008 PES General Meeting July 20-24, 2008.
- [5] *Insulation co-ordination. IV: Computational guide to insulation co-ordination and modeling of electrical networks*, IEC 60071-4, 2004.
- [6] CIGRE WG 33.10, "Temporary overvoltage withstand characteristics of extra high voltage equipment", Electra 179, 1998, p. 38-49.
- [7] CIGRE WG 33.10 "Temporary Overvoltages. Test Case Results", Electra 188, 2000.
- [8] CIGRE WG 33.02, *Guidelines for representation of network elements when calculating transients*: CIGRE Brochure 39, 1990.
- [9] A. Gole, J.A. Martinez, and A. Keri (eds.), "Modeling and Analysis of Power System Transients Using Digital Programs", IEEE Special Publication TP-133-0, 1999.
- [10] J.A. Martinez, Mork, B.A., "Transformer modeling for low- and mid-frequency transients - A review", Power Delivery, IEEE Transactions on, Volume 20, Issue 2, April 2005 Page(s): 1625 – 1632.
- [11] IEEE Slow Transients TF of IEEE WG on Modelling and Analysis of Systems Transients Using Digital Programs, "Modelling and Analysis Guidelines for Slow Transients : Part III. The Study of Ferroresonance", IEEE Trans. on Power Delivery, vol. 15, no. 1, January 2000.
- [12] B.A. Mork, F. Gonzalez, D. Ishchenko, D. L. Stuehm, J. Mitra, "Hybrid Transformer Model for Transient Simulation-Part I: Development and Parameters", IEEE Trans. Power Delivery, Vol. 22, pp. 248-255, 2007.
- [13] B.A. Mork, F. Gonzalez, D. Ishchenko, D. L. Stuehm, J. Mitra, "Hybrid Transformer Model for Transient Simulation-Part II: Laboratory Measurements and Benchmarking", IEEE Trans. Power Delivery, Vol. 22, pp. 256-262, Jan. 2007.
- [14] H. W. Domme, EMTP Theory Book, Vancouver, Canada, Microtran Power System Analysis Corporation, 1992.
- [15] *Rotating electrical machines 4: Methods for determining synchronous machine quantities from tests*, IEC standard 60034-4, 2008.
- [16] IEEE PES Task Force on Data for Modeling System Transients, "Parameter determination for modeling system transients: Part I. Overhead Lines", IEEE Transactions on Power Delivery, Vol. 20, No. 3, 2005, p. 2038-2044.
- [17] IEEE PES Task Force on Data for Modeling System Transients, "Parameter determination for modeling system transients: Part I.II Transformers", IEEE Transactions on Power Delivery, Vol. 20, No. 3, 2005, p. 2051-2062.
- [18] M. J. Heathcote, *The J&P Transformer Book*, 13th ed. New York: Newnes, 2007.
- [19] F. de León and A. Semlyen, "Time domain modelling of eddy current effects for transformer transients," IEEE Trans. Power Del., vol. 8, no. 1, pp. 271–280, Jan. 1993.
- [20] E. E. Fuchs, D. Yildirim, and W. M. Grady, "Measurement of eddy current loss coefficient P_{EC-R} , derating of single-phase transformers, and comparison with K-factor approach," IEEE Trans. Power Del., vol. 15, no. 1, pp. 148–154, Jan. 2000.
- [21] CIGRE Working Group 13.03, "Switching overvoltages in EHV and UHV systems with special reference to closing and reclosing transmission lines", Electra, 30, oct. 1973, p. 70-122.
- [22] E. J. Tarasiewicz, A. S. Morched, A. Narang, and E. P. Dick, "Frequency dependent eddy current models for nonlinear iron cores", IEEE Trans. Power Syst., vol. 8, no. 2, pp. 588–597, May 1993.

IX. BIOGRAPHY



Manuel Martínez Duró was born in Lleida, Spain, in 1975. He received the electrical engineering degree from the Universitat Politècnica de Catalunya, Barcelona, Spain, in 1999. He joined Electricité de France, R&D Division, France, in 2001.